

Oil-source correlation of Lower-Triassic oil seepages in Ni'erguan village, Southern Guizhou Depression, China

Fang Yuan^{1,2} · Yuhong Liao¹ · Yunxin Fang^{1,3} · Ansong Geng¹

Received: 28 November 2014/Revised: 25 May 2015/Accepted: 19 October 2015/Published online: 28 October 2015
© Science Press, Institute of Geochemistry, CAS and Springer-Verlag Berlin Heidelberg 2015

Abstract There are abundant bitumens and oil seepages stored in vugs in a Lower-Triassic Daye formation (T₁d) marlite in Ni'erguan village in the Southern Guizhou Depression. However, the source of those oil seepages has not been determined to date. Multiple suites of source rocks of different ages exist in the depression. Both the oil seepages and potential source rocks have undergone complicated secondary alterations, which have added to the difficulty of an oil-source correlation. For example, the main source rock, a Lower-Cambrian Niutitang Formation (Є₁n) mudstone, is over mature, and other potential source rocks, both from the Permian and the Triassic, are still in the oil window. In addition, the T₁d oil seepages underwent a large amount of biodegradation. To minimize the influence of biodegradation and thermal maturation, special methods were employed in this oil-source correlation study. These methods included catalytic hydrolysis, to release covalently bound biomarkers from the over mature kerogen of Є₁n mudstone, sequential extraction, to obtain chloroform bitumen A and chloroform bitumen C from the T₁d marlite, and anhydrous pyrolysis, to release pyrolysates from the kerogen of T₁d marlite. Using the methods above, the biomarkers and *n*-alkanes released

from the oil samples and source rocks were analysed by GC–MS and GC-C-IRMS. The oil-source correlation indicated that the T₁d oil seepage primarily originated from the Є₁n mudstone and was partially mixed with oil generated from the T₁d marlite. Furthermore, the seepage also demonstrated that the above methods were effective for the complicated oil-source correlation in the Southern Guizhou Depression.

Keywords Oil seepage · Biomarker · Carbon isotopic composition · Catalytic hydrolysis · Oil-source correlation

1 Introduction

The Southern Guizhou Depression is located in the southern region of the Guizhou Province in Southwest China. This depression covers an area of approximately 30,000 km². The Southern Guizhou Depression experienced a multi-stage tectonic orogeny (Xu et al. 2010). The depression came into being in the Caledonian and Hercynian orogeny, which was followed by the uplift and deformation of the eastern part of the depression during the Indosinian and Yanshanian orogeny. Thereafter, intense tectonic deformation in the Himalayas led to the exposure of the Lower Paleozoic strata. Oil seepage occurs in many of the strata in the northern part of the depression (Fig. 1).

Considerable research has been conducted on the oil-source correlation of the oil seepages in the Southern Guizhou Depression. For example, the Є₁n mudstone was considered to be the source of the Middle-Cambrian oil seepages in Gedong town, the Middle-Ordovician oil seepages in Huzhuang village, the Middle-Ordovician oil seepages and the Lower Middle-Silurian oil seepages in

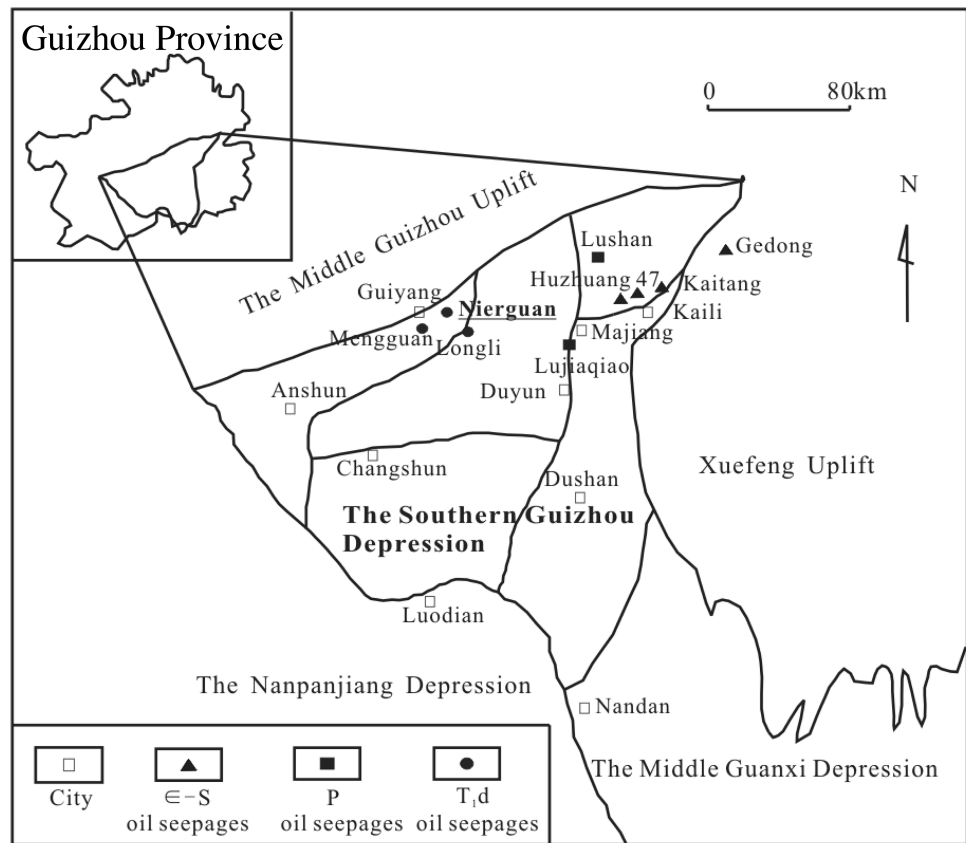
✉ Ansong Geng
asgeng@gzb.ac.cn

¹ The State Key Laboratory of Organic Geochemistry, Guangzhou Institute of Geochemistry, Chinese Academy of Sciences, Wushan, Guangzhou 510640, People's Republic of China

² University of Chinese Academy of Sciences, Beijing 100039, People's Republic of China

³ The Key Laboratory of Marine Mineral Resources, Guangzhou Marine Geological Survey, Ministry of Land and Resources, Guangzhou 510075, People's Republic of China

Fig. 1 Map showing locations of oil seepages (modified from He et al. 2012)



Kaitang town (Zhang et al. 2007; Pan and Liu 2009; Fang et al. 2011). However, the Lower-Permian oil seepages in Lujiaqiao village and Lushan town were thought to be originated from the P₁q mudstone (Zhang et al. 2007; Peng et al. 2011; He et al. 2012; Huang et al. 2013). Nevertheless, the source of the T₁d oil seepages is still under debate. Fu et al. (2007) proposed that the source of the T₁d oil seepages in Ni'erguan village was the P₁q mudstone because the bulk $\delta^{13}\text{C}$ values of the T₁d oil seepages are similar to those of the P₁q mudstone in the Kaili area. However, after comparing the aromatic hydrocarbons of the T₁d oil seepages with those in the Middle-Ordovician oil seepages in Huzhuang village and Kaitang town, He et al. (2012, 2013) proposed that the E₁n mudstone was the source of all of the T₁d oil seepages near Mengguan town (Fig. 1). Peng et al. (2011) argued that the T₁d oil seepages in the nearby Paomuchong village of Longli county were a mixture generated from both Lower-Cambrian and Lower-Permian source rocks, as they found that the distribution of saturated hydrocarbons and regular steranes in the T₁d oil seepages of Longli county were similar to those in the P₁q mudstone in the Kaili area, while the bulk $\delta^{13}\text{C}$ values of the T₁d oil seepages were close to those of the Middle-Ordovician oil seepages in Huzhuang village. Moreover, Zhao (2000) thought that the T₁d marlite could be the

source of the T₁d oil seepages because of its moderate maturity (the R_0 was approximately 0.7 %) and high TOC content (up to 5.7 %).

Oil-source correlation is difficult in the study area because of the following three factors. First, the E₁n mudstone is over mature, resulting in low yields of extractable organic matter (EOM). Furthermore, free biomarkers in the EOM might have been significantly altered by severe thermal maturation and may not effectively reflect the geochemical information of the original organic matter. Second, the reservoir (the T₁d marlite) is still in the oil-generative window and has considerable petroleum generation potential. Therefore, the EOM from T₁d may be mixed with oils of different origins. Third, the T₁d oil seepages have undergone a large amount of biodegradation. The distribution of the biomarkers might have been altered during biodegradation and some biomarker parameters may be invalid for an oil-source correlation. Therefore, special methods must be applied in an oil-source rock correlation study. These methods include catalytic hydrolysis, to release covalently bound biomarkers from the kerogen of E₁n mudstone, sequential extraction, to obtain chloroform bitumen A and chloroform bitumen C from the T₁d marlite, and anhydrous pyrolysis, to release the pyrolysates from the kerogen of T₁d marlite.

The covalently bound biomarkers released by catalytic hydrolysis (HyPy) were less affected by thermal maturation (Love et al. 1995, 1998; Murray et al. 1998; Liao et al. 2012; Wu et al. 2012; Fang et al. 2014) and contamination during outcrop exposure (Wu et al. 2013). Much of the original geochemical information about the source of the organic matter was preserved by covalently bound biomarkers, due to the protection of kerogen macromolecules. Therefore, HyPy experiments were performed for the over-mature E_{1n} mudstone. Three types of sedimentary organic matter (i.e., adsorbed, included and crystal-enclosed organic matter) exist in carbonate rock (Gehman 1962; Fu and Jia 1984). The adsorbed organic matter and chloroform bitumen A was directly extracted by chloroform. After the removal of the chloroform bitumen A and the subsequent acid treatment of the minerals, the included and crystal-enclosed organic matter in the mineral crystals and inclusions were obtained by Soxhlet extraction with chloroform; this extract is termed chloroform bitumen C (Fu and Liu 1982, Fu and Jia 1984; Xie et al. 2000, 2004). Numerous previous studies have indicated that the molecular signature of the initial oil charge could be effectively revealed with a geochemical analysis of oil, bearing fluid inclusions and the sequential extraction of oil reservoir rocks (Karlsen et al. 1993; Wilhelms et al. 1996; George et al. 1997, 1998, 2004; Schwark et al. 1997; Leythaeuser et al. 2000, 2007; Pan and Yang 2000; Pan et al. 2000, 2003, 2005, 2007; Pan and Liu 2009; Gong et al. 2007). In the present study, the T_{1d} marlite was subjected to a practical sequential extraction method to recover the free, adsorbed (Bitm-A) and inclusion (Bitm-C) oils from the oil reservoir rocks to reconstruct the filling history of the oil reservoirs in Ni'erguan village. The T_{1d} kerogen was heated to 320 °C for 72 h in a quartz tube to acquire the anhydrous pyrolysates that reflect the original geochemical characteristics of the T_{1d} marlite.

The purpose of this study was to use special methods, including catalytic hydrolysis, sequential extraction and anhydrous pyrolysis, to make an oil-source correlation for the T_{1d} oil seepage. The oil-source correlation between the T_{1d} oil seepages and the potential source rocks was based on biomarker parameters, carbon isotope composition and the petroleum geological settings.

2 General geological settings

The Southern Guizhou Depression developed many sedimentary formations from the Sinian to the Triassic. Multiple suites of source rocks exist primarily in the depression (Tenger et al. 2008). The main source rock, the Lower-Cambrian Niutitang Formation (E_{1n}), occurs everywhere in

the depression and consists of approximately 103 m of dark mudstone with a high TOC (total organic carbon) content (average 3.16 %). This rock's kerogen is composed of sapropelic components and is at the over mature stage. The secondary source rock, the Lower-Permian Qixia Formation (P_{1q}), mainly occurs in the Majiang-Kaili area. The P_{1q} source rock consists of dark-grey limestone and intercalates with mudstone, usually with a total thickness of 70–175 m and a TOC content ranging from 0.55 % to 1.89 %. The P_{1q} source rock with a high TOC content occurs only in the Kaili area—the TOC contents of some samples can reach 2.0 %. The kerogen of P_{1q} is at the mature stage. However, to the west, the lithology of the P_{1q} stratum gradually shifts to grey micrite limestone. The P_{1q} stratum near the Ni'erguan village has a total thickness of ≤ 20 m and a TOC content of ≤ 0.5 %. Therefore, the hydrocarbon generation potential of the P_{1q} source rocks is poor around the Ni'erguan village, although a number of researchers insist that the P_{1q} source rocks should be considered in an oil-source rock correlation. The Lower-Triassic Daye Formation (T_{1d}) marlite is constrained to a 20 to 60 km wide zone, which is south of the Anshun-Guiyang area and has a thickness of 30 to 123 m and a TOC content typically ranging from 0.4 % to 1.2 %. However, the TOC content of the marlite can reach 5.6 % near Guiyang, which is very close to the Ni'erguan village. The maturity of the T_{1d} marlite is still in the oil-generative window. Thus, the T_{1d} marlite has considerable petroleum generation potential. Therefore, various source rocks were collected and analysed in the oil-source correlation study.

3 Samples and experimental

3.1 Samples

Two samples were collected from the geologic outcrop of the Ni'erguan village, including the Lower-Triassic Daye Formation (T_{1d}) oil seepage and the Lower-Triassic Daye Formation marlite. The other two samples, the Lower-Permian Qixia Formation (P_{1q}) mudstone and the Lower-Cambrian Niutitang Formation (E_{1n}) mudstone were collected from the Majiang-Kaili area. More details about the source rocks of the P_{1q} mudstone and the E_{1n} mudstone can be found in Fang et al. (2011). The basic geochemical characteristics of samples are listed in Table 1.

The oil seepage sample Oil-1 is stored in vugs of the Lower-Triassic Daye Formation (T_{1d}) marlite. The T_{1d} marlite sample NEG-3 is still in the oil window, with a TOC value of 0.87 % and a T_{max} of 442 °C. The E_{1n} mudstone sample SW-8 is over mature, with a TOC of 6.44 % and a T_{max} of 609 °C. The P_{1q} mudstone sample

Table 1 Basic geochemical parameters of samples

Sample	Formation	Description	$\delta^{13}\text{C}$ (‰)	TOC (%)	S1	S2	HI	T_{max} (°C)
Oil-1	T ₁ d	Oil seepage	−30.5	–	–	–	–	–
NEG-3	T ₁ d	Marlite	−26.8	0.87	0.67	2.59	298	442
SW-8*	E ₁ n	Mudstone	−32.5	6.44	–	–	2	609
WC-3*	P ₁ q	Mudstone	−28.7	2.01	–	–	130	449

* The same as Fang et al. (2011)

WC-3 is still in the oil window, with a TOC value of 2.01 % and T_{max} of 449 °C.

3.2 Experimental

The T₁d marlite (NEG-3) sample was crushed to 80 mesh and extracted with a mixture of dichloromethane (DCM) and methanol (93:7, v/v) for 72 h to collect the chloroform bitumen A (Bitm-A). The residue of the NEG-3 sample was cleaned with dilute hydrochloric acid (1:4, v/v) to dissolve the carbonate mineral, and then extracted with a mixture of dichloromethane (DCM) and methanol (93:7, v/v) for 72 h to obtain the chloroform bitumen C (Bitm-C). Finally, the Soxhlet extracted kerogen was sealed in a glass tube under nitrogen and heated at 320 °C for 72 h for anhydrous pyrolysis. After cooling, the pyrolysates (Bitm-Py) were obtained by ultrasonic extraction, using a mixture of dichloromethane (DCM) and methanol (93:7, v/v).

After the E₁n mudstone and P₁q mudstone samples were extracted, the HyPy experiment was conducted on the kerogen of E₁n mudstone sample SW-8 using procedures previously described by Love et al. (1995), Liao et al. (2012), Wu et al. (2012, 2013) and Fang et al. (2014).

Before the HyPy experiment, the kerogen of E₁n mudstone was extracted with a mixture of benzene/acetone/methanol (5:5:2, v/v/v) for 1 week. An aqueous solution of ammonium dioxodithiomolybdate [(NH₄)₂MoO₂S₂] was added to the extracted kerogen to give a nominal loading of molybdenum of ca. 5 wt%. A sample with a catalyst was loaded into the HyPy reactor tube. The system was under a constant H₂ pressure of 15.0 MPa and a hydrogen flow of 4 l/min. Next, this reactor tube was heated from an ambient temperature to 300 °C (5 min) at 250 °C/min. Next, we replaced the silica trap and heated the tube again from ambient temperature to 250 °C at 300 °C/min and from 250 to 520 °C (5 min) at 8 °C/min thereafter. The hydrolysis product was collected in a silica trap and cooled with liquid nitrogen.

The asphaltenes were precipitated from the oil seepage and source rock extracts. The maltenes were separated into saturated, aromatic and polar (NSO) fractions. The saturated and aromatic hydrocarbon fractions were analysed by GC–MS. The GC–C–IRMS system was used to measure the $\delta^{13}\text{C}$ values of the *n*-alkanes in the saturated fraction.

Before the GC–C–IRMS analysis, the saturated hydrocarbon fractions were depleted of branched/cyclic hydrocarbons according to the procedures of urea adduction described by Liao et al. (2004).

3.3 Instruments

The GC–MS analysis of the saturated and aromatic biomarkers was performed using a Finnigan Trace GC Ultra gas chromatograph coupled with a Thermo Fisher DSQ II mass spectrometer. The column used was a HP-1 fused silica capillary column (60 m × 0.32 mm × 0.25 μm i.d.). When the saturated hydrocarbons were analysed, the GC oven was held isothermally at 60 °C for 2 min, programmed to 295 °C at 4 °C/min and then remained at this temperature for 30 min. The temperature program for analysing the aromatic biomarkers was set initially at 60 °C for 2 min, programmed to 290 °C at a rate of 3 °C/min and held for 25 min. The ion-source temperature was 250 °C. The GC–MS system was operated in the electron impact (EI) mode with electron energy of 70 eV.

The VG Isochrom II GC–C–IRMS system was used to determine the $\delta^{13}\text{C}$ values of the individual *n*-alkanes. The column used a fused silica capillary column (DB-1; 30 m × 0.32 mm × 0.25 μm i.d.). Helium was the carrier gas and CO₂ was used as a reference gas. The GC oven was set isothermally at 80 °C for 2 min, programmed to 295 °C at 6 °C/min and then held for 25 min. The combustion furnace was held at 850 °C. The standard deviation of the GC–C–IRMS for each measurement was less than 0.2 ‰.

4 Results and discussion

4.1 Geochemical characteristics of samples

4.1.1 The geochemical characteristics of potential source rocks

The total yields of the hydrolysis products (H-SW-8) by HyPy from E₁n mudstone kerogen SW-8 were 40 times greater than those of the extracts (SW-8), which suggests that HyPy can release a higher amount of soluble organic matter from over mature kerogen than the Soxhlet

extraction from the corresponding source rock can (Liao et al. 2012; Fang et al. 2014). Fang et al. (2014) already carefully compared the covalently bound biomarkers and the free biomarkers in the EOM of SW-8 and determined that the covalently bound biomarkers released by HyPy were more stable and provided more dependable information for oil-source correlation. The GC–MS TIC trace of the saturated hydrocarbon in the extracts (SW-8) showed the unimodal arrangement with a maximum at n -C₁₈ (Fig. 2). However, the GC–MS TIC trace of the saturated hydrocarbon fraction of H-SW-8 showed a high relative abundance of branched alkanes (Fig. 2). The distribution of C₂₇–C₂₉- $\alpha\alpha\alpha$ R steranes in the H-SW-8 was C₂₇ > C₂₉ \geq C₂₈, which was similar to that of the extracts (Fig. 3). However, in the extracts, the abundance of pregnane and homopregnane were higher than those of regular steranes and the pregnane/regular steranes ratio was greater than that of the hydropyrolysates (Fang et al. 2014). The

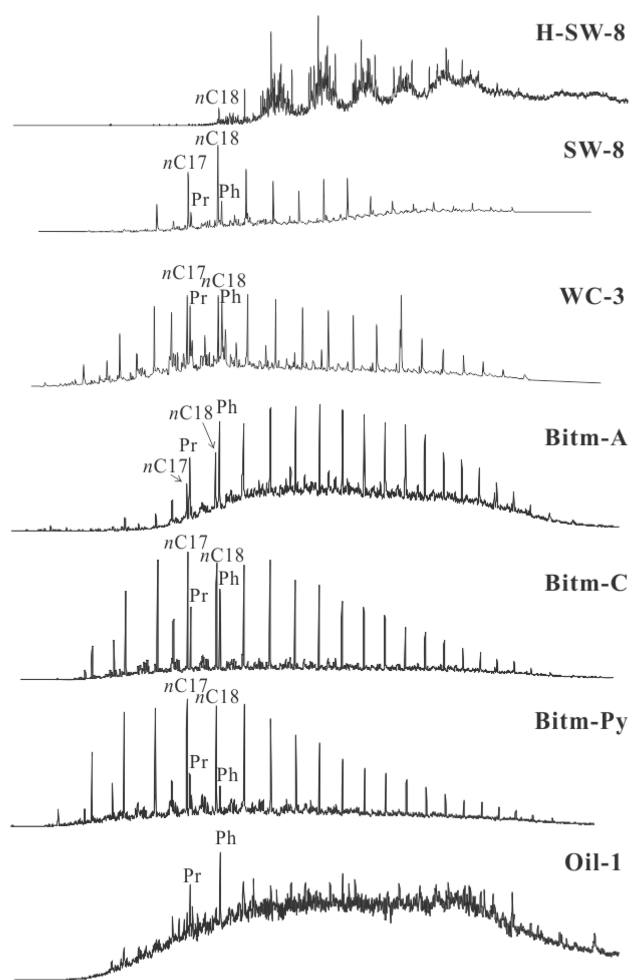
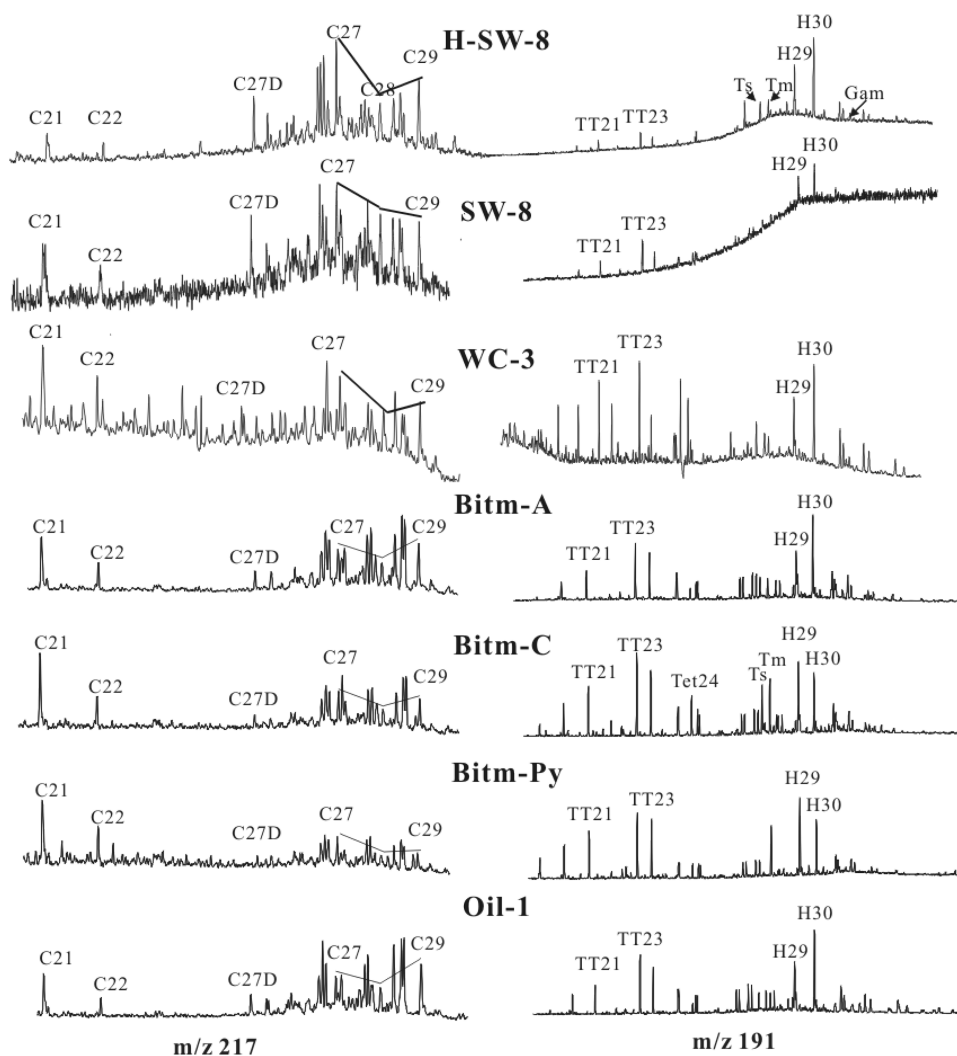


Fig. 2 TICs of saturated hydrocarbons in the hydropyrolysates, Soxhlet extracts, sequential extracts, anhydrous pyrolysates and oil seepage. 1 n C17 = C₁₇- n -alkanes, 2 n C18 = C₁₈- n -alkanes, 3 Pr = Pristane, 4 Ph = Phytane

abundance of pregnane and homopregnane was increased relative to that of the regular steranes, with an increase in thermal maturity (Huang et al. 1994). Therefore, the thermal maturity of the hydropyrolysates is lower than that of the extracts. In the hydropyrolysates, the distribution of terpanes was characterized by a high content of C₃₀ hopane and a low content of tricyclic terpanes, while the distribution in the extracts was the opposite (Fig. 3). With an increase in thermal maturity, the abundance of the tricyclic terpanes gradually increased relative to that of the hopanes, as the thermal stability of the tricyclic terpanes is higher than that of the hopanes (Peters et al. 1995). This finding also implies that, unlike the free biomarkers, the hydropyrolysates are insensitive to thermal alteration (Liao et al. 2012). Therefore, the covalently bound biomarkers released by HyPy could retain more effective information concerning the original organic input than the free biomarkers could. The GC–MS TIC trace of the saturated compounds in the Soxhlet extract of the P_{1q} mudstone (WC-3) showed a unimodal arrangement and a maximum of n -C₁₈ (Fig. 2). The chromatogram of m/z 217 was dominated by pregnane and homopregnane. The distribution of C₂₇–C₂₈–C₂₉ regular steranes was characterized by C₂₉ > C₂₈ > C₂₇ (Fig. 3), while the chromatogram of m/z 191 was predominantly characterized by C₂₃ tricyclic terpane (Fig. 3). Thus, the characteristics of the C_{1n} mudstone extract and the P_{1q} mudstone extract are markedly different.

There was an unresolved complex mixture (UCM) hump in the GC–MS TIC trace of saturated hydrocarbons in the chloroform bitumen A from T_{1d} marlite (Bitm-A). Additionally, the concentration of pristane and phytane was higher in the entire sample relative to n -C₁₇ and n -C₁₈, respectively (Fig. 2). This could imply that the chloroform bitumen A has undergone slight biodegradation (Peters and Moldowan, 1993). However, the n -alkane distribution still had a unimodal arrangement and a maximum at n -C₂₂. The distribution of C₂₇–C₂₈–C₂₉- $\alpha\alpha\alpha$ R steranes had an order of C₂₉ > C₂₇ > C₂₈. The pentacyclic terpanes were characterized by a high abundance of C₃₀ hopane, while the C₂₃ tricyclic terpane was predominant in the tricyclic terpanes (Fig. 3). Nevertheless, in the chloroform bitumen C (Bitm-C) of the T_{1d} marlite, there was no unresolved complex mixture (UCM) hump, and the distribution of the n -alkanes showed an unimodal arrangement and a maximum at n -C₁₇ (Fig. 2). Chloroform bitumen C generally enters the mineral crystal inclusions or gaps during early diagenesis, and was therefore less affected by the thermal alteration and modern sediment pollution than free oil and adsorbed oil because of the mineral crystal's protection (Spiro 1984). Therefore, bitumen C might preserve information about the original organic matter (Spiro 1984; Wen and Zhang 1997;

Fig. 3 m/z 217 and m/z 191 mass chromatograms of the hydropyrolysates, Soxhlet extracts, sequential extracts, anhydrous pyrolysates and oil seepage. 1 TT21 = C_{21} -tricyclic terpane, 2 TT23 = C_{23} -tricyclic terpane, 3 Tet24 = C_{24} -tetracyclic terpane, 4 Ts = $18\alpha(H)$ - C_{27} -trisnorhopane, 5 Tm = $17\alpha(H)$ - C_{27} -trisnorhopane, 6 H29 = C_{29} - $\alpha\beta$ hopane, 7 H30 = C_{30} - $\alpha\beta$ hopane, 8 C21 = C_{21} -pregnane, 9 C22 = C_{22} -homopregnane, 10 C27D = C_{27} - $\beta\alpha S$ diasterane, 11 C27 = C_{27} - $\alpha\alpha\alpha R$ sterane, 12 C28 = C_{28} - $\alpha\alpha\alpha R$ sterane, 13 C29 = C_{29} - $\alpha\alpha\alpha R$ sterane



Li et al. 2008). By comparing the geochemical characteristics of chloroform bitumen A and chloroform bitumen C, we can find the differences in the source of the organics and might be able to confirm the time of hydrocarbon filling (Pan et al. 2003; Pan and Liu 2009; Jin et al. 2012). In Bitm-C, the abundance of C_{27} - $\alpha\alpha\alpha R$ sterane was slightly higher than that of the C_{28} - $\alpha\alpha\alpha R$ and C_{29} - $\alpha\alpha\alpha R$ steranes. Additionally, the terpane distribution was characterized by a high abundance of C_{23} tricyclic terpane and C_{29} hopane relative to C_{30} hopane (Fig. 3). Therefore, Bitm-C was distinctly different from Bitm-A in the distributions of both steranes and terpanes. Anhydrous pyrolysis of kerogen releases strongly bound constituents from kerogen, such as n -alkanes and biomarkers (Tissot and Welte 1984; Brian 1984; Colin and Wang 1988). Anhydrous pyrolysis at 320 °C for 72 h is a type of mild pyrolysis, during which abundant hydrocarbons can be released without significantly affecting the biomarker distribution and the carbon isotopes (Fu and Qin, 1995; Xiong and Geng, 2000). The

GC-MS TIC trace of saturates in the pyrolysates (Bitm-Py) had a maximum at n - C_{17} (Fig. 2). The C_{27} - $\alpha\alpha\alpha R$ sterane was most abundant among the C_{27} - C_{29} - $\alpha\alpha\alpha R$ steranes in Bitm-Py. The C_{29} hopane was the most abundant compound in the distribution of terpanes in Bitm-Py. We found the same results for Bitm-C (Fig. 3). Therefore, remarkable differences exist between Bitm-A, Bitm-C and Bitm-Py. The C_{29} - $\alpha\alpha\alpha R$ sterane was the most abundant compound among the C_{27} - C_{29} - $\alpha\alpha\alpha R$ steranes in Bitm-A, but in Bitm-C and Bitm-Py, the distribution of C_{27} - C_{29} - $\alpha\alpha\alpha R$ steranes was dominated by the C_{27} - $\alpha\alpha\alpha R$ sterane. C_{30} hopane was higher than C_{29} hopane in Bitm-A, but C_{29} hopane was higher in Bitm-C and Bitm-Py.

4.1.2 The geochemical characteristics of the T₁d oil seepage

The GC-MS TIC trace of saturates in the T₁d oil seepage (Oil-1) showed that most n -alkanes were removed and that

there was a broad unresolved complex mixture (UCM) hump and high peaks, indicating pristane and phytane (Fig. 2). This suggests that the oil seepage Oil-1 was heavily biodegraded (Peters and Moldowan 1993). The concentration of regular steranes was higher than that of pregnane and homopregnane, but the distribution of steranes was dominated by the C_{29} - $\alpha\alpha\alpha$ R sterane (Fig. 3), indicating that the distribution of C_{27} - C_{28} - C_{29} - $\alpha\alpha\alpha$ R steranes might have been altered to some extent by biodegradation. Similar to Bitm-A, Oil-1 had a normal pattern and C_{30} hopane predominated in the pentacyclic terpanes, while C_{23} tricyclic terpane predominated in the tricyclic terpanes (Fig. 3).

4.2 Oil-source correlation of the T₁d oil seepages with possible potential source rocks

4.2.1 Steranes

The distribution of the C_{27} - C_{28} - C_{29} regular steranes was widely used in oil-source correlations due to the stability of regular steranes in the oil window (Peters et al. 1989). The distribution of the C_{27} - C_{28} - C_{29} regular steranes in the hydropyrolysates H-SW-8 was dominated by the C_{27} - $\alpha\alpha$ R sterane (Fig. 4A), while in the EOM from the P₁q mudstone WC-3, it was dominated by the C_{29} - $\alpha\alpha\alpha$ R sterane. For the T₁d marlite, the C_{27} - $\alpha\alpha\alpha$ R sterane was most abundant in the distribution of C_{27} - C_{29} - $\alpha\alpha\alpha$ R steranes in chloroform bitumen C (Bitm-C) and the kerogen pyrolysates (Bitm-Py). Nevertheless, the distribution of the C_{27} - C_{29} - $\alpha\alpha\alpha$ R regular steranes in the T₁d oil seepage (Oil-1) was dominated by the C_{29} - $\alpha\alpha\alpha$ R sterane. The $C_{29}/(C_{27} + C_{28} + C_{29})$ ratio was higher than 0.54, much higher than that in the potential source rocks mentioned above. Diasteranes are thought to have a higher bioresistance than the C_{27-29} regular steranes (Rullkötter and Wendisch 1982; Goodwin et al. 1981). The C_{27} D $\beta\alpha$ R diasterane/ C_{27} $\alpha\alpha$ R sterane ratio in Oil-1 was 0.94, which was higher than those in the other samples (Fig. 4B). The broad unresolved complex mixture (UCM) hump of the T₁d oil seepage indicates that biodegradation had partly consumed the C_{27} - $\alpha\alpha\alpha$ R and C_{28} - $\alpha\alpha\alpha$ R steranes in Oil-1 but

had not yet affected the C_{29} - $\alpha\alpha\alpha$ R sterane and the C_{27} D $\beta\alpha$ S diasterane. Therefore, the biodegradation may have invalidated the biomarker parameters based on the regular steranes in the T₁d oil seepage for the oil-source correlation. The regular sterane characteristics of the T₁d oil seepage for the oil-source correlations should be cautiously applied.

It is believed that pregnane and homopregnane were derived from hormones, pregnanol, pregnanone or the thermal cracking of the C_{27} - C_{29} -regular steranes (De Leeuw and Bass 1986; Huang et al. 1994). Pregnane and homopregnane are highly resistant to biodegradation and may preserve original information about the source organic matter (Wenger and Isaksen 2002). Table 2 shows that the pregnane/homopregnane ratio (C_{21}/C_{22}) of H-SW-8 and WC-3 is 1.78 and 1.51, respectively. The C_{21}/C_{22} ratio in Bitm-C and Bitm-Py is 2.93 and 2.66, respectively. The ratio in Oil-1 is 2.12, lower than Bitm-C and Bitm-Py, but higher than H-SW-8 and WC-3. Therefore, the heavily biodegraded oil seepage Oil-1 may have multiple sources.

4.2.2 Terpanes

The bioresistance of the terpanes was higher than that of the regular steranes. The abundances of the terpanes was high relative to that of the regular steranes in the T₁d oil seepage, indicating biodegradation may not have affected the distribution of the terpanes (Seifert and Moldowan 1979; Aquino et al. 1983; Peters and Moldowan 1993) in the T₁d oil seepage. Therefore, the characteristics of terpanes could be used for oil-source correlation. Tricyclic terpanes are widely found in oils and source rock extracts, especially in crude oils from marine sources. The tricyclic terpanes possibly originated from prokaryotic cell membranes and are generally dominated by C_{23} tricyclic terpane (Ourisson et al. 1982; Connan et al. 1980; Aquino et al. 1983). The T₁d oil seepage (Oil-1), chloroform bitumen A (Bitm-A) and chloroform bitumen C (Bitm-C), all contained high concentrations of tricyclic terpanes, with similar distributions of tricyclic terpanes (Table 2). For Oil-1, Bitm-A and Bitm-C, the ratio of C_{21} tricyclic terpane to C_{23} tricyclic terpane (TT_{21}/TT_{23}) ranged from 0.52 to 0.59,

Fig. 4 Triangular plot of the distribution of C_{27} - C_{28} - C_{29} $\alpha\alpha\alpha$ R steranes and C_{27} D $\beta\alpha$ R diasterane/ C_{27} $\alpha\alpha$ R sterane ratio in the hydropyrolysates, Soxhlet extracts, sequential extracts, anhydrous pyrolysates and oil seepages

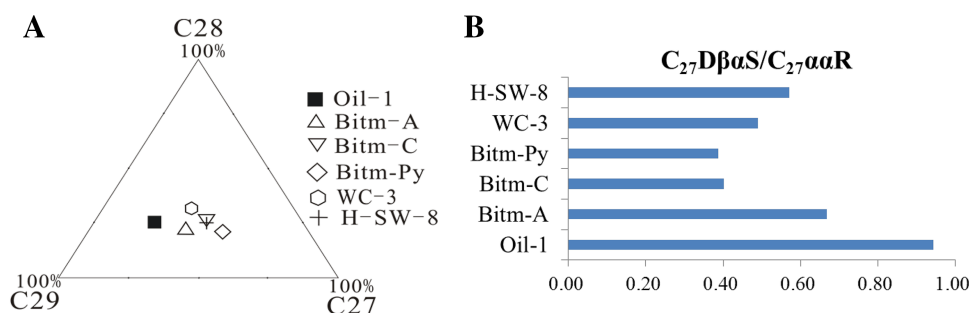


Table 2 Biomarker parameters of the hydropyrolysates, the Soxhlet extracts, the sequential extracts, the pyrolysates and the oil seepage

Sample	1	2	3	4	5	6	7	8	9	10	11	12	13	14	15
Oil-1	0.52	1.24	0.52	0.08	0.46	0.49	0.66	0.59	2.12	0.19	0.27	0.54	0.51	0.94	0.76
Bitm-A	0.56	1.16	0.62	0.13	0.48	0.55	0.61	0.72	2.29	0.32	0.24	0.45	0.64	0.67	0.86
Bitm-C	0.59	1.31	1.35	0.66	0.45	1.12	0.57	0.69	2.93	0.37	0.28	0.35	0.64	0.40	0.87
Bitm-Py	0.71	1.13	1.18	0.25	0.11	1.50	0.60	0.66	2.66	0.46	0.23	0.32	0.58	0.39	0.99
WC-3	0.75	1.52	1.63	–	0.56	0.41	0.63	–	1.51	0.31	0.32	0.37	0.37	0.49	1.58
H-SW-8*	0.60	1.8	0.14	–	0.55	0.59	0.59	–	1.78	0.38	0.27	0.36	0.41	0.57	2.03

1 C_{21}/C_{23} tricyclic terpane, 2 C_{23}/C_{24} tricyclic terpane, 3 C_{23} tricyclic terpane/ C_{30} hopane, 4 C_{24} tetracyclic terpane/ C_{30} hopane, 5 $Ts/(Ts + Tm)$, 6 C_{29}/C_{30} hopane, 7 $22S/(22S + 22R)-C_{31}$ homohopane, 8 $22S/(22S + 22R)-C_{32}$ homohopane, 9 pregnane/homopregnane, 10 $C_{27}-\alpha\alpha\alpha R/(C_{27}-\alpha\alpha\alpha R + C_{28}-\alpha\alpha\alpha R + C_{29}-\alpha\alpha\alpha R)$, 11 $C_{28}-\alpha\alpha\alpha R/(C_{27}-\alpha\alpha\alpha R + C_{28}-\alpha\alpha\alpha R + C_{29}-\alpha\alpha\alpha R)$, 12 $C_{29}-\alpha\alpha\alpha R/(C_{27}-\alpha\alpha\alpha R + C_{28}-\alpha\alpha\alpha R + C_{29}-\alpha\alpha\alpha R)$, 13 $\beta\beta/(\alpha\alpha + \beta\beta)-C_{29}$ sterane, 14 C_{29} $D\beta\alpha S$ diasterane/ $C_{27}\alpha\alpha R$ sterane, 15 $MPI = 1.5 * (3\text{-methylphenanthrene} + 2\text{-methylphenanthrene}) / (\text{phenanthrene} + 9\text{-methylphenanthrene} + 1\text{-methylphenanthrene})$

* Hydropyrolysis products of kerogen from SW-8

while the ratio of C_{23} tricyclic terpane to C_{24} tricyclic terpane (TT_{23}/TT_{24}) ranged from 1.16 to 1.31 (Fig. 5A, B). The TT_{21}/TT_{23} ratios in the EOM from the P_{1q} mudstone (WC-3), C_{1n} kerogen hydropyrolysates (H-SW-8) and the T_{1d} kerogen pyrolysates (Bitm-Py) are 0.75, 0.60 and 0.71, respectively, while it is 0.52 in Oil-1 (Fig. 5A). Therefore, the TT_{21}/TT_{23} ratio of the T_{1d} oil seepage might have a close relationship with C_{1n} mudstone. A simulation study by Liao et al. (2012) indicated that the $TT_{23}/(TT_{23} + TT_{24})$ ratio is a reliable index in bitumen–source and bitumen–bitumen correlations when oils have undergone heavy biodegradation and subsequent severe thermal alteration. Table 2 shows the TT_{23}/TT_{24} ratios in oil seepages, bitumen C, potential source rock extracts, kerogen hydropyrolysates and kerogen pyrolysates. The TT_{23}/TT_{24} ratio of Oil-1 was much closer to that of T_{1d} kerogen pyrolysate Bitm-Py ($TT_{23}/TT_{24} = 1.13$) than those of H-SW-8 and WC-3 (Fig. 5B), indicating that the T_{1d} oil seepage Oil-1 might have a close relationship with the T_{1d} mudstone. Therefore, the distribution of tricyclic terpanes shows that the T_{1d} oil seepage might come from multiple source rocks.

The ratio of C_{23} tricyclic terpane to C_{30} pentacyclic terpane (TT_{23}/H_{30}) was commonly used as a source-related biomarker parameter to identify the different organic inputs from bacteria, algae or other prokaryotic organisms (Peters et al. 2005; Liao et al. 2012). The TT_{23}/H_{30} ratios in the chloroform bitumen A (Bitm-A) from the T_{1d} marlite and the T_{1d} oil seepage Oil-1 were 0.62 and 0.52, respectively. The TT_{23}/H_{30} ratio in H-SW-8 was only 0.14, lower than that in Oil-1 (Fig. 5C). Nevertheless, the TT_{23}/H_{30} ratios in the other potential source rock samples were greater than 1.0. Hence, the TT_{23}/H_{30} ratio of Oil-1 falls between those of H-SW-8 and Bitm-Py, indicating that the T_{1d} oil seepage should originate from multiple source rocks.

The H_{29}/H_{30} ratios in crude oils were usually below 1.0, except for crude oils derived from evaporite or carbonate. The crude oils generated from source rocks containing rich terrestrial organic matter also exhibited a relative predominance of C_{29} hopane. Therefore, the H_{29}/H_{30} ratio might contain information regarding the original organic input and the depositional environment of the source rocks (Clark and Philp 1989; Brooks 1986). Figure 5D shows that the T_{1d} kerogen pyrolysate Bitm-Py has the highest H_{29}/H_{30} ratio of 1.50, while the Bitm-C has second highest H_{29}/H_{30} value, 1.12. Nevertheless, the H_{29}/H_{30} ratio for the T_{1d} oil seepage is 0.49, which is very similar to those of the extracts and hydropyrolysates from the potential source rocks, but is significantly lower than those of Bitm-Py and Bitm-C (Fig. 5D). Therefore, some differences should be evident in the source organic input of the T_{1d} oil seepage and the T_{1d} marlite.

A number of maturity parameters are listed in Table 2. Most of the maturity parameters were similar for all of the samples, such as $22S/(22S + 22R)-H_{31}$. However, the $Ts/(Ts + Tm)$ ratios of all of the samples, except Bitm-Py, were very close. Bitm-Py had a much lower $Ts/(Ts + Tm)$ ratio of 0.11 (Fig. 5E), possibly because the covalently bound biomarkers were protected from secondary alterations, such as biodegradation and thermal maturation, by the kerogen macromolecular structure. Ts and Tm are thought to be bonded to the kerogen macromolecules in early diagenesis. They can avoid the isomerization common in free biomarkers (Love et al. 1998; Liao et al. 2012). The MPI indices of Oil-1, Bitm-A, Bitm-C and Bitm-Py had similar values, all within the range of 0.76–0.99 (Fig. 5F). However, the MPI indices of WC-3 and H-SW-8 were 1.58 and 2.03, respectively (Fig. 5F), both greater than that of Oil-1 and Bitm-Py, implying that the T_{1d} oil seepage may correlate with the T_{1d} marlite.

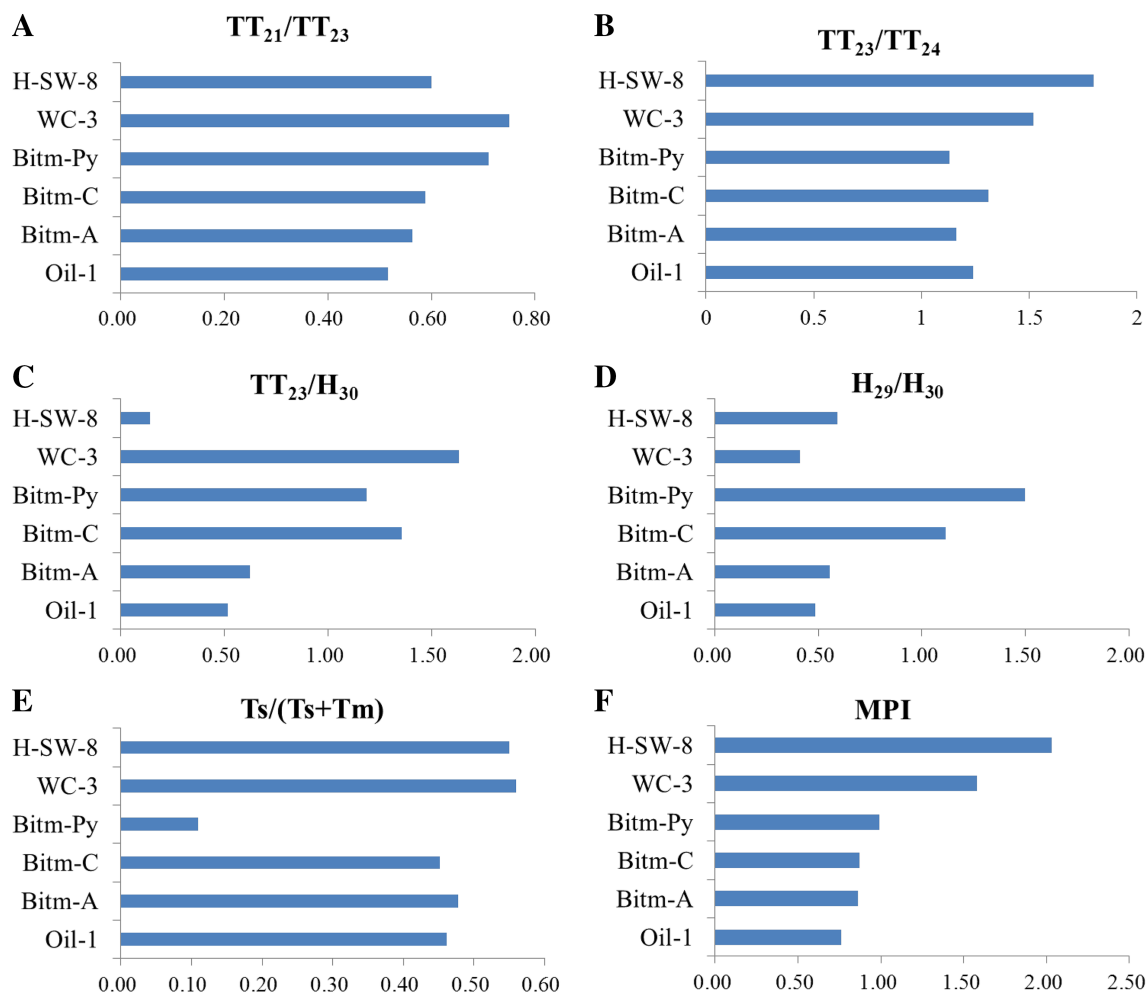


Fig. 5 Biomarker parameters of terpanes in the hydropyrollysates, Soxhlet extracts, sequential extracts, anhydrous pyrollysates and oil seepage

The above oil-source correlation study based on the distribution of tricyclic terpanes and pentacyclic triterpanes suggests that the T_{1d} oil seepage could not have been generated from a single source rock. Not only the T_{1d} marlite, but also the E_{1n} mudstone might have contributed to the oil seepage in the T_{1d} marlite. Furthermore, because of the characteristics of the steranes and terpanes, the possibility of a contribution from the P_{1q} source rock cannot be excluded.

4.2.3 Triaromatic steroids

It is commonly known that triaromatic steroids are the aromatization products of monoaromatic steranes and have highest bioreistance among the commonly used biomarkers (Peters and Moldowan 1993; Ludwig et al. 1981). The long chain triaromatic steroids (C₂₆–C₂₈-triaromatic steroid) could have originated from marine Acritarchs (Zhang et al. 2002; Peters et al. 2005). The distribution of long chain triaromatic steroids can reflect

the original organic input (Ludwig et al. 1981; Mackenzie et al., 1982). The short chain triaromatic steroids (C₂₀–C₂₁-triaromatic steroid) did not originate entirely from the degradation of their long chain homologues (C₂₆–C₂₈-triaromatic steroid), ergo they may have different organic matter inputs than those of the long chain homologues (Mackenzie et al. 1982; Riolo et al. 1986; Beach et al. 1989). Therefore, it is appropriate to consider the distribution of the long chain triaromatic steroids in an oil-source correlation. Figure 6 shows that the distribution of long chain triaromatic steroids in the T_{1d} oil seepage Oil-1 is dominated by the C₂₈-triaromatic steroid, which is different from the distributions in the Bitm-Py, but similar to those of the Lower Ordovician oil seepages (KT-1, KT-2) in Kaitang village in the Kaili area, which were demonstrated to have originated from the E_{1n} mudstone by Fang et al. (2011). Therefore, the T_{1d} oil seepage should have a close relationship with the E_{1n} mudstone. By comparing the distribution of the triaromatic steroids, He et al. (2012) also proposed that the T_{1d} oil seepages in Mengguan

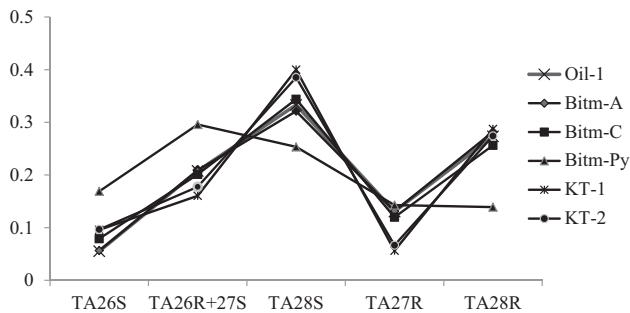


Fig. 6 Distributions of long chain triaromatic steroids in the sequential extracts, pyrolysates and oil seepages. *TA26S* C₂₆S-triaromatic steroid, *TA26R + 27S* C₂₆R-triaromatic steroid + C₂₇S-triaromatic steroid, *TA28S* C₂₈S-triaromatic steroid, *TA27R* C₂₇R-triaromatic steroid, *TA28R* C₂₈R-triaromatic steroid

township, which was very close to Ni'erguan village, originated from the E_{1n} mudstone. Additionally, the triaromatic steroids were not detected in the P_{1q} mudstone, indicating that the P_{1q} source rock cannot be the sole source rock for the T_{1d} oil seepage.

4.2.4 Bulk $\delta^{13}C$ values of whole oil samples and extracts

The bulk $\delta^{13}C$ for both the potential source rock kerogens and the oil seepage are shown in Table 1. The bulk kerogen $\delta^{13}C$ values of the T_{1d} marlite (NEG-3), E_{1n} mudstone (SW-8) and P_{1q} mudstone (WC-3) were -26.8‰ , -32.5‰ and -28.7‰ , respectively. The bulk $\delta^{13}C$ value of the T_{1d} oil seepage (Oil-1) was -30.5‰ , while the chloroform bitumen A (Bitm-A) and chloroform bitumen C (Bitm-C) from T_{1d} marlite had similar $\delta^{13}C$ values of -29.6‰ and -29.4‰ , respectively, approximately 1 ‰ heavier (enriched in ^{13}C) than that of Oil-1. The bulk $\delta^{13}C$ value of whole oil changes very little and could be a useful index in an oil-source correlation of heavily biodegraded oils (Kvenvolden et al. 1995; Sun et al. 2005). If the kerogen pyrolysates, chloroform bitumen C, chloroform bitumen A and oil seepage originated from the same source rock, the difference between them in the bulk $\delta^{13}C$ should be within 2 ‰ (Tissot and Welte, 1984). However, the $\delta^{13}C$ value of Bitm-Py was -27.8‰ , 2.7 ‰ heavier than that of the T_{1d} oil seepage (Fig. 7). Therefore, the T_{1d} oil seepage could not be entirely derived from the T_{1d} marlite, but might partly originate from the E_{1n} mudstone whose bulk $\delta^{13}C$ of kerogen is -32.5‰ . Additionally, the bulk $\delta^{13}C$ values of two oil seepages (Hu47, MJ-02) derived from the E_{1n} mudstone (Zhang et al. 2007) were -30.8‰ and -31.9‰ , respectively (Table 3; Fig. 7), close to that of the T_{1d} oil seepage. This implies that the T_{1d} oil seepage could mainly originate from the E_{1n} mudstone. The bulk $\delta^{13}C$ values of the Lower Permian oil seepages (MJ-03, LJ-22) that are believed to have originated from the high

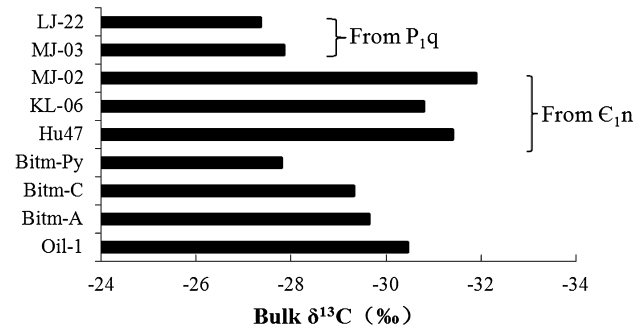


Fig. 7 Bulk $\delta^{13}C$ values of the whole oil seepages, sequential extracts and anhydrous pyrolysates

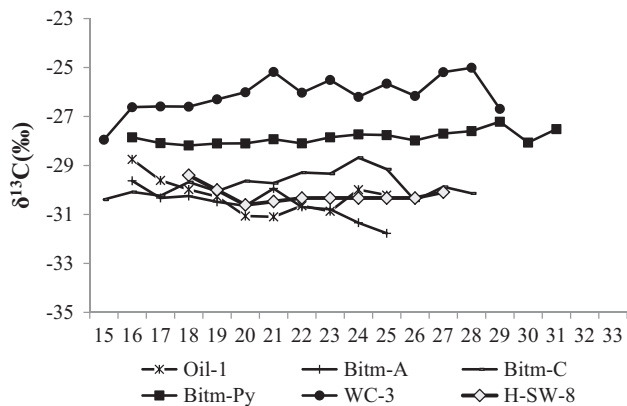
quality P_{1q} source rocks are about -27.5‰ (Table 3; Fig. 7), which is significantly heavier than that of the T_{1d} oil seepage (Oil-1). Therefore, the T_{1d} oil seepage cannot have a close relationship with the P_{1q} source rocks.

4.2.5 The $\delta^{13}C$ values of individual *n*-alkanes

The stable carbon isotopic composition of the individual *n*-alkanes is one of the most important pieces of information for an oil-source correlation (Bjørøy et al. 1991; Liu et al. 2006; Yu et al. 2012). It is commonly accepted that the $\delta^{13}C$ values of *n*-alkanes change only slightly during biodegradation (Xiong and Geng 2000; Sun et al. 2005). Mild thermal maturation may lead to a slight enrichment in ^{13}C . Typically, such a variation in the $\delta^{13}C$ value is within 2–3 ‰ (Bjørøy et al. 1992; Liao et al. 2004, 2012; Liao and Geng 2009). The $\delta^{13}C$ value for the individual *n*-alkanes in the T_{1d} oil seepage (Oil-1) ranged from -29‰ to -31.5‰ , which is very similar to those in the chloroform bitumen A (Bitm-A) (Fig. 8; Table 4). The $\delta^{13}C$ value of the individual *n*-alkanes (C₁₈–C₂₇) in Bitm-C ranged from -29‰ to -30‰ , heavier than those in both Oil-1 and Bitm-A. This indicates that exchange between free oil (Oil-1) and adsorbed oil (Bitm-A) might easily occur, but that such an exchange would be difficult between free oil and oil trapped in an inclusion. The $\delta^{13}C$ values of the individual *n*-alkanes in Bitm-Py were all around -28‰ , which was 1–2 ‰ heavier than those in Bitm-C. However, the difference in the $\delta^{13}C$ of the individual *n*-alkanes between Bitm-Py and Oil-1 was over 2 ‰ (Fig. 8), indicating that the T_{1d} oil seepage could not be entirely derived from the T_{1d} marlite. The $\delta^{13}C$ values of the individual *n*-alkanes in the EOM from the P_{1q} mudstone (WC-3) were the heaviest, ranging from -25‰ to -28‰ (Fig. 8), while the $\delta^{13}C$ values of individual *n*-alkanes in the hydropyrolysates (H-SW-8) ranged from -29‰ to -31‰ (Fang et al. 2014), very similar to those in Oil-1 (Fig. 8), suggesting that the T_{1d} oil seepage could be mostly generated from the E_{1n} mudstone.

Table 3 Basic information of oil seepages from other literatures

Sample	Description	Location	Formation	$\delta^{13}\text{C}$ (‰)	Source	From article
KT-1	Oil seepage	Kaitang	O ₁ h	−32.2	Є ₁ n	Fang et al. (2011)
KT-2	Oil seepage	Kaitang	O ₁ h	−32.3	Є ₁ n	
Hu47	Oil seepage	Kaiki	O ₁ h	−31.4	Є ₁ n	Zhang et al. (2007)
KL-06	Oil seepage	Luomiao	S ₁₋₂ w	−30.8	Є ₁ n	
MJ-02	Oil seepage	Majiang	O ₁ h	−31.9	Є ₁ n	
MJ-03	Oil seepage	Majiang	P ₁ m	−27.85	P ₁ q	
LJ-22	Oil seepage	Lujiaqiao	P ₁ m	−27.36	P ₁ q	

**Fig. 8** $\delta^{13}\text{C}$ values of individual *n*-alkanes in the hydropyrolysates, Soxhlet extracts, sequential extracts, anhydrous pyrolysates and oil seepage

Above all, biodegradation may have invalidated the biomarker parameters based on the regular steranes in the T₁d oil seepage. The distributions of pregnane,

homopregnane, tricyclic terpanes and pentacyclic triterpanes suggested that the T₁d oil seepage could have originated from multiple source rocks. The T₁d marlite and the Є₁n mudstone might have contributed to the oil seepage. However, according to the distribution of the long chain triaromatic steroids, the bulk $\delta^{13}\text{C}$ value and the $\delta^{13}\text{C}$ value of individual *n*-alkanes, the T₁d oil seepage was similar to oils generated from the Є₁n mudstone and was notably different than the oils generated from the P₁q source rock, which implies the T₁d oil seepage is primarily generated from the Є₁n mudstone and the partially mixed oils derived from the T₁d marlite.

4.3 The history of hydrocarbon generation of source rocks

Figure 9 shows the history of the hydrocarbon generation of source rocks in this area. The Є₁n mudstone entered the oil generative window between the Late Cambrian and the Early Ordovician, and then was quickly uplifted, resulting

Table 4 The $\delta^{13}\text{C}$ values of individual *n*-alkanes of the hydropyrolysates, the Soxhlet extracts, the sequential extracts, the pyrolysates and the oil seepage

Carbon number	Sample					
	Oil-1	Bitm-A	Bitm-C	Bitm-Py	WC-3	H-SW-8
15			−30.39		−27.95	
16	−28.75	−29.63	−30.08	−27.85	−26.62	
17	−29.61	−30.33	−30.24	−28.09	−26.59	
18	−29.98	−30.25	−29.68	−28.18	−26.60	−29.40
19	−30.27	−30.48	−30.05	−28.10	−26.30	−30.00
20	−31.07	−30.65	−29.64	−28.10	−26.01	−30.61
21	−31.10	−29.94	−29.72	−27.93	−25.18	−30.47
22	−30.64	−30.69	−29.29	−28.10	−26.03	−30.33
23	−30.87	−30.79	−29.34	−27.85	−25.51	−30.33
24	−29.99	−31.34	−28.68	−27.73	−26.20	−30.33
25	−30.21	−31.77	−29.15	−27.76	−25.66	−30.33
26			−30.43	−27.98	−26.16	−30.33
27			−29.87	−27.70	−25.19	−30.09
28			−30.14	−27.60	−25.01	
29				−27.22	−26.69	
30				−28.06		
31				−27.52		

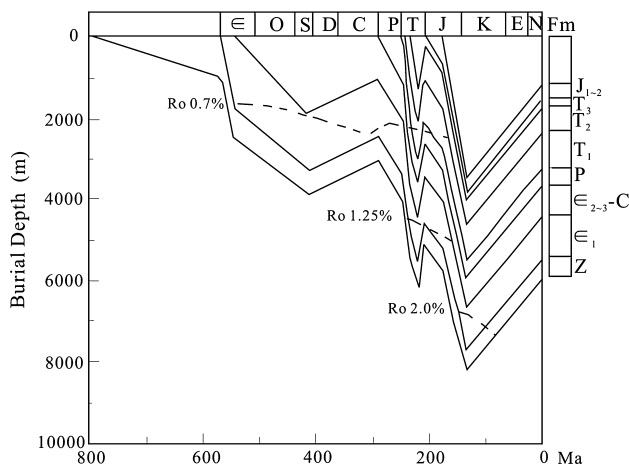


Fig. 9 Hydrocarbon generation history of source rocks in Guiyang area (modified from Feng et al. 2008)

in the erosion of the Ordovician and Silurian strata (Ma et al. 2004; Gao and Liu 2008; Feng et al. 2008). Thereafter a slow uplifting in the study area lasted until the Early Permian. Subsequently, the burial depth of the E_1n mudstone kept increasing and the maximum burial depth exceeded 6000 m in the Indosinian orogeny, resulting in a secondary hydrocarbon generation in the E_1n mudstone and the formation of faults. Meanwhile, the T_1d marlite was in its early diagenesis stage. The oil generated by the E_1n mudstone was expelled and quickly migrated into gaps in the T_1d marlite through the faults, in addition to being partly trapped in the mineral crystal inclusions as chloroform bitumen C. The P_1q mudstone entered the oil generative window during the Triassic, but the high-quality P_1q source rocks only occurred in the Majiang-Kaili area. Both the TOC and thickness indicate that the P_1q source rocks have a very low petroleum potential in the study area. The oil generated from the high-quality P_1q source rocks could not have migrated over the long distance from the Majiang-Kaili area to the Ni'erguan village. Therefore, the P_1q micrite limestone in the Ni'erguan village could not have contributed to the T_1d oil seepage. However, if the T_1d marlite generated a small amount of oils in the Jurassic, it might be a secondary source of the T_1d oil seepage in the Ni'erguan village. Therefore, the T_1d oil seepage might be a mixture of oils generated from both the E_1n mudstone and the T_1d marlite.

5 Conclusions

(1) Our oil-source correlation results indicate that the heavily biodegraded T_1d oil seepage was primarily generated from the E_1n mudstone in the Late Permian-Early Triassic and partially mixed with oil generated from T_1d

marlite, but the oil generated from the P_1q may have been neglected;

(2) Our oil-source correlation in Ni'erguan village demonstrates that such methods as catalytic hydroxyprolysis, anhydrous pyrolysis and sequential extraction are effective in a complicated oil-source correlation in the Southern Guizhou Depression.

Acknowledgments We would like to extend our thanks to Dr. Liangliang Wu and Dr. Bin Cheng of Guangzhou Institute of Geochemistry for their useful suggestions and help. Our thanks also go to Dr. Yankuang Tian and Mr. Huashan Chen of Guangzhou Institute of Geochemistry for their help with the GC-MS and GC-C-IRMS analyses. This work was supported jointly by the National Science and Technology Major Project of China (Grant Nos: 2011ZX05008-002 and 2011ZX05005-001).

References

- Aquino Neto FR, Trendel JM, Restle A, Connan J, Albrecht PA (1983) Occurrence and formation of tricyclic and tetracyclic terpanes in sediments and petroleum. In: Bjorøy M et al (eds) *Advances in organic geochemistry*. Wiley, Chichester, pp 659–667
- Beach F, Peakman TM, Abbott GD, Sleeman R, Maxwell JR (1989) Laboratory thermal alteration of triaromatic steroid hydrocarbons. *Org Geochem* 14:109–111
- Bjorøy M, Hall K, Gillyon P, Jumeau J (1991) Carbon isotope variation in n-alkanes and isoprenoids of whole oils. *Chem Geol* 93:13–20
- Bjorøy M, Hall PB, Hustad E, Williams JA (1992) Variation in stable carbon isotope ratios of individual hydrocarbons as a function of artificial maturity. *Org Geochem* 19:89–105
- Brian H (1984) Pyrolysis studies and petroleum exploration. *Adv Pet Geochem* 1:247–298
- Brooks PW (1986) Unusual biological marker geochemistry of oils and possible source rocks, offshore Beaufort-Mackenzie Delta, Canada. *Org Geochem* 10:401–406
- Clark JP, Philp RP (1989) Geochemical characterization of evaporate and carbonate depositional environments and correlation of associated crude oils in the Black Creek Basin, Alberta. *Can Pet Geol Bull* 37:401–416
- Colin B, Wang LJ (1988) Application of pyrolysis in petroleum geochemistry: a bibliography. *Anal Appl Pyrol* 13:9–81
- Connan J, Restle A, Albrecht P (1980) Biodegradation of crude oil in the Aquitaine basin. *Phys Chem Earth* 12:1–17
- De Leeuw JW, Bass M (1986) Early diagenesis of steroids. In: Johns RB (ed) *Biological markers in the sedimentary record*. Elsevier, Amsterdam, pp 102–127
- Fang YX, Liao YH, Wu LL, Geng AS (2011) Oil-source correlation for the paleo-reservoir in the Majiang area and remnant reservoir in the Kaili area, South China. *J Asian Sci* 41:147–158
- Fang YX, Liao YH, Wu LL, Geng AS (2014) The origin of solid bitumen in the Honghuayuan Formatin (O1 h) of the Majiang paleo-reservoir-Evidence from catalytic hydroxyprolysis. *Org Geochem* 68:107–117
- Feng CM, Niu XS, Wu CL (2008) A study of hydrocarbon fluid inclusions in Qianzhong uplift and its adjacent areas. *Acta Petrologica et Mineralogica* 27:121–126
- Fu JM, Jia RF (1984) Main forms of disseminated organic matter in carbonate rocks, their evolutionary characteristics and significance in oil-gas evolution. *Geochimica* 1:1–9 (in Chinese with English abstract)

- Fu JM, Liu DH (1982) Some characteristics of the evolution of organic matter in carbonate formations. *Acta Pet Sin* 1:1–9
- Fu JM, Qin KZ (1995) The kerogen geochemistry. Guangzhou Science and Technology Publishing House, Guangzhou, pp 471–515
- Fu XD, Liang DG, Chen JP, Zhao Z, Bian LZ, Zhang SC, Zhong NN, Xie ZY, Xu ZB (2007) The effective hydrocarbon source rocks evaluation in complex tectonic area, South China, pp 518–519. (Report from Sinopec Exploration Southern Company, in Chinese)
- Gao L, Liu GX (2008) Analysis oil source of Lower Palaeozoic crude oil from Kaili area in Guizhou province. *Pet Geol Exp* 30:186–191
- Gehman HMJ (1962) Organic matter in limestones. *Geochim Cosmochim Acta* 26:885–893
- George SC, Krieger FW, Eadington PJ, Quezada RA, Greenwood PF, Eisenberg LI, Hamilton PJ, Wilson MA (1997) Geochemical comparison of oil-bearing fluid inclusions and produced oil from the Toro sandstone, Papua New Guinea. *Org Geochem* 26:155–173
- George SC, Lisk M, Summons RE, Quezada RA (1998) Constraining the oil charge history of the South Pepper oil field from the analysis of oil-bearing fluid inclusions. *Org Geochem* 29:631–648
- George SC, Ahmed M, Liu K, Volk H (2004) The analysis of oil trapped during secondary migration. *Org Geochem* 35:1489–1511
- Gong S, George SC, Volk H, Liu K, Peng P (2007) Petroleum charge history in the Lunnan Low Uplift, Tarim Basin, China—evidence from oil-bearing fluid inclusions. *Org Geochem* 38:1341–1355
- Goodwin NS, Park PJD, Rawlinson T (1981) Crude oil biodegradation under simulated and natural conditions. In: Bjørøy M et al (eds) *Advances in organic geochemistry*. Wiley, New York, pp 650–658
- He XY, Yao GS, Cai CF, Shen AJ, Wu JW, Huang L, Chen ZL (2012) Aromatic hydrocarbons distribution in oil seepages from the southern Guizhou Depression, SW China: Geochemical characteristics and geological implications. *Geochimica* 41:442–451
- He XY, Cai CF, Yao GS, Xiong XH, Shen AJ, Xiang L, Wu JW (2013) Origins of oil seepages in the southern Guizhou Depression, SW China: evidence from carbon isotopes, sulfur isotopes and biomarkers. *Acta Pet Sin* 29:1059–1072
- Huang DF, Zhang DJ, Li JC (1994) The origin of 4-methyl steranes and pregnanes from tertiary strata in the Qaidam Basin, China. *Org Geochem* 22:343–348
- Huang L, Li Y, Li GJ, Xu ZY, Xiong SY, Li C (2013) Geochemical characteristics and origin of Ordovician well crude oil and oil seepages from limestone fractures and vugs in Kaili area, southeastern Guizhou. *Mar Orig Pet Geol* 18:19–25
- Jin XD, Pan CC, Yu S, Qin JZ (2012) Molecular geochemistry of solid bitumen-bearing carbonate reservoir rocks from the Puguang Gas Field and nearby areas. *Geochimica* 41:293–302
- Karlsen DA, Nedkvitne T, Larter SR, Bjørlykke K (1993) Hydrocarbon composition of authigenic inclusions: application to elucidation of petroleum reservoir filling history. *Geochim Cosmochim Acta* 57:3641–3659
- Kvenvolden KA, Hostettler FD, Carlson PR, Rapp JB, Threlkeld CN, Warden A (1995) Ubiquitous tar balls with a California-source signature on the shorelines of Prince William Sound, Alaska. *Environ Sci Technol* 29:2684–2694
- Leythaeuser D, Schwark L, Keuser C (2000) Geological conditions and geochemical effects of secondary petroleum migration and accumulation. *Mar Pet Geol* 17:857–859
- Leythaeuser D, Keuser C, Schwark L (2007) Molecular memory effects recording the accumulation history of petroleum reservoirs: a case study of the Heidrun Field, offshore Norway. *Mar Pet Geol* 24:199–220
- Li YX, Geng AS, Liu JP, Xiong YQ (2008) Organic geochemical characteristics of the Lower Palaeozoic carbonate rocks in the Huanghua Depression, the Bohai Bay Basin. *Pet Geol Exp* 30:75–81
- Liao YH, Geng AS (2009) Stable carbon isotopic fractionation of individual *n*-alkanes accompanying primary migration: Evidence from hydrocarbon generation–expulsion simulations of selected terrestrial source rocks. *Appl Geochem* 24:2123–2132
- Liao YH, Geng AS, Xiong YQ, Liu DH, Lu JL, Liu JP, Zhang HZ, Geng XH (2004) The influence of hydrocarbon expulsion on carbon isotopic composition of individual *n*-alkanes in pyrolysates of selected terrestrial kerogens. *Org Geochem* 35:1479–1488
- Liao YH, Fang YX, Wu LL, Geng AS, Hsu SC (2012) The characteristics of the biomarkers and $\delta^{13}\text{C}$ of *n*-alkanes released from thermally altered solid bitumens at various maturities by catalytic hydroxyprolysis. *Org Geochem* 46:56–65
- Liu JP, Geng AS, Xiong YQ (2006) The application of stable carbon and hydrogen isotopic compositions of individual *n*-alkanes to Paleozoic oil/source rock correlation enigmas in the Huanghua depression, China. *J Petrol Sci Eng* 54:70–78
- Love GD, Snape CE, Carr AD, Houghton RC (1995) Release of covalently-bound alkane biomarkers in high yields from kerogen via catalytic hydroxyprolysis. *Org Geochem* 23:981–986
- Love GD, Snape CE, Fallick AE (1998) Differences in the mode of incorporation and biogenicity of the principle aliphatic constituents of a Type I oil shale. *Org Geochem* 28:797–811
- Ludwing B, Hussler G, Wehrung P, Albrecht P (1981) $\text{C}_{20}\text{--}\text{C}_{29}$ triaromatic steroid derivatives in sediments and petroleum. *Tetrahedron Lett* 22:3313–3316
- Ma L, Chen HJ, Gan KW, Xu KD, Xu XS, Wu GY, Ye Z, Lian X, Wu SH, Qiu WY, Zhang PL (2004) Geotectonic and petroleum geology of marine sedimentary rocks in southern China. Geological Publishing House, Beijing, pp 513–534
- Mackenzie AS, Lamb NA, Maxwell JR (1982) Steroid hydrocarbons and the thermal history of sediments. *Nature* 295:223–226
- Murray AP, Love GD, Snape CE, Bailey JL (1998) Comparison of covalently-bound aliphatic biomarkers released via hydroxyprolysis with their solvent-extractable counterparts for a suite of Kimmeridge clays. *Org Geochem* 29:1487–1505
- Ouirisson G, Albrecht P, Rohmer M (1982) Predictive microbial biochemistry, from molecular fossils to prokaryotic membranes. *Trends Biochem Sci* 3:236–239
- Pan CC, Liu DY (2009) Molecular correlation of free oil, adsorbed oil and inclusion oil of reservoir rocks in the Tazhong Uplift of the Tarim Basin, China. *Org Geochem* 40:387–399
- Pan CC, Yang JP (2000) Geochemical characteristics and implications of hydrocarbons in reservoir rocks of Junggar Basin, China. *Chem Geol* 167:321–335
- Pan CC, Fu J, Sheng G (2000) Sequential extraction and compositional analysis of oil-bearing fluid inclusions in reservoir rocks from Kuche Depression, Tarim Basin. *Chin Sci Bull* 45:60–66
- Pan CC, Yang JQ, Fu JM, Sheng GY (2003) Molecular correlation of free oil and inclusion oil of reservoir rocks in the Junggar Basin, China. *Org Geochem* 34:357–374
- Pan CC, Feng JH, Tan YM, Yu LP, Luo XP, Sheng GY, Fu JM (2005) Interaction of oil components and clay minerals in reservoir sandstones. *Org Geochem* 36:633–654
- Pan CC, Tan YM, Feng JH, Jin GX, Zhang YX, Sheng GY, Fu JM (2007) Mixing and biodegradation of hydrocarbons in the Daerqi oilfield, Baiyinchagan Depression, northern China. *Org Geochem* 38:1479–1500
- Peng JN, Liu GX, Luo KP, Lv JX (2011) Analysis of oil and source rock correlation and pooling history in Kaili area. *J Southwest Pet Univ (Science & Technology Edition)* 33:61–66
- Peters KE, Moldowan JM (1993) The biomarker guide: interpreting molecular fossils in petroleum and ancient sediments. Prentice Hall, New Jersey, pp 182–363
- Peters KE, Moldowan JM, Driscoll AR (1989) Origin of Beatrice oil by co-sourcing from Devonian and Middle Jurassic source rocks, Inner Moray Firth, U.K. *Am Assoc Pet Geol Bull* 73:454–471

- Peters KE, Clark ME, Das Gupta U, Mcaffrey MA, Lee CY (1995) Recognition of an InfraCambrian source rock based on biomarkers in the Baghewala-1 Oil, India. *Am Assoc Pet Geol Bull* 79:1481–1494
- Peters KE, Walters CC, Moldowan JM (2005) *The biomarker guide II: biomarkers and isotopes in petroleum systems and earth history*. Cambridge University Press, Cambridge, pp 698–699
- Riolo J, Hussler G, Albrecht P, Connan J (1986) Distribution of aromatic steroids in geological samples: their evaluation as geochemical parameters. *Org Geochem* 10:981–990
- Rullkötter J, Wendisch D (1982) Microbial alteration of 17 α (H)-hopane in Madagascar asphalts: removal of C-10 methyl group and ring opening. *Geochim Cosmochim Acta* 46:1543–1553
- Schwark L, Stoddart D, Keuser C, Spitthoff B, Leythaeuser D (1997) A novel sequential extraction system for whole core plug extraction in a solvent flow-through cell—application to extraction of residual petroleum from an intact pore-system in secondary migration studies. *Org Geochem* 26:19–31
- Seifert WK, Moldowan JM (1979) The effect of biodegradation on steranes and terpanes in crude oils. *Geochim Cosmochim Acta* 43:111–126
- Spiro B (1984) Effects of the mineral matrix on the distribution of geochemical markers in thermally affected sedimentary sequences. *Org Geochem* 6:543–559
- Sun YG, Chen ZY, Xu SP, Cai PX (2005) Stable carbon and hydrogen isotopic fractionation of individual n-alkanes accompanying biodegradation: evidence from a group of progressively biodegraded oils. *Org Geochem* 36:225–238
- Tenger, Qin JZ, Zheng LJ (2008) Hydrocarbon potential on excellent hydrocarbon source rock in southern Guizhou depression and its special-temporal distribution. *Acta Geol Sinica* 82:366–372
- Tissot BP, Welte DH (1984) *Petroleum formation and occurrence*. Springer, Berlin, pp 225–238
- Wen ZG, Zhang AY (1997) Biomarker characteristics of bitumen A and bitumen C of Ordovician carbonate rocks in Ordos basin. *Geoscience* 11:197–202
- Wenger LM, Isaksen GH (2002) Control of hydrocarbon seepage intensity on level of biodegradation in sea bottom sediments. *Org Geochem* 33:1277–1292
- Wilhelms A, Horstad I, Karlsen D (1996) Sequential extraction—a useful tool for reservoir geochemistry. *Org Geochem* 24:1157–1172
- Wu LL, Liao YH, Fang YX, Geng AS (2012) The study on the source of the oil seeps and bitumens in the Tianjingshan structure of the northern Longmen Mountain structure of Sichuan Basin, China. *Mar Pet Geol* 37:147–161
- Wu LL, Liao YH, Fang YX, Geng AS (2013) The comparison of biomarkers released by hydrolysis and by Soxhlet extraction from source rocks of different maturities. *Chin Sci Bull* 58:373–383
- Xie QL, Zhou ZY, Lu MY (2000) Organic matter enclosed in carbonate minerals—a kind of important hydrocarbon-producing matter. *Acta Miner Sin* 20:59–61
- Xie QL, Zhou ZY, Shi JX, Zhu YX (2004) Classification and characteristics of hydrocarbon regeneration from the Lower Palaeozoic Group in the Tazhong area of Tarim Basin. *Geol Rev* 50:377–383
- Xiong YQ, Geng AS (2000) Carbon isotopic composition of individual n-alkanes in asphaltene pyrolysates of biodegraded crude oils from the Liaohe Basin, China. *Org Geochem* 31:1441–1449
- Xu ZY, Yao GS, Guo QX, Chen Z, Dong Y, Wang PW, Ma LQ (2010) Genetic interpretation about geotectonic and structural transfiguration of the Southern Guizhou Depression. *Geotectonica et Metallogenia* 34:20–31
- Yu S, Pan CC, Wang JL, Jin XD, Jiang LL, Liu DY, Lv XX, Qin JZ, Qian YX, Ding Y, Chen HH (2012) Correlation of crude oils and oil components from reservoirs and source rocks using carbon isotopic compositions of individual n-alkanes in the Tazhong and Tabei Uplift of the Tarim Basin, China. *Org Geochem* 31:1441–1449
- Zhang SC, Moldowan JM, Li MW, Bian LZ, Zhang BM, Wang FY, He ZH, Wang D (2002) The abnormal distribution of the molecular fossils in the Pre-Cambrian and Cambrian: its biological significance. *Sci China (Series D)*. 45:3–10
- Zhang Q, Tenger, Qin ZR (2007) Oil source of oil seepage and solid bitumen in Kaili–Majiang area. *Acta Geol Sin* 81:1118–1124
- Zhao L (2000) Restitution of organic matter type in marine-facing oil source rock in Guizhou–Yunnan–Guangxi area. *Guizhou Geol* 17:86–90